Molecular dynamics simulations of anomalous relaxation in a binary Lennard-Jones system

Susumu Fujiwara* and Fumiko Yonezawa
Department of Physics, Keio University, 3-14-1 Hiyoshi, Kohoku-ku, Yokohama 223, Japan
(Received 20 March 1995)

The anomalous relaxation in normal and supercooled liquids is studied by molecular-dynamics (MD) simulations of a simple Lennard-Jones binary mixture for various temperatures and wave numbers. Our MD simulations show that the anomalous structural relaxation of a stretched-exponential type appears not only in a supercooled liquid region but also in a normal liquid region. This fact indicates that the anomalous relaxation is not a feature characteristic of supercooled liquids alone, but rather it is a phenomenon to be found in broader categories of disordered systems. [S1063-651X(96)05507-9]

PACS number(s): 61.25.−f, 61.20.Ja, 61.20.Lc

I. INTRODUCTION

The anomalous relaxation, which was discovered about 150 years ago [1], is a long-standing problem. Recently, much attention has been given to this problem since state-of-the-art experimental techniques have made it possible to observe the anomalous relaxation in a wide variety of phenomena such as the structural relaxation in supercooled liquids [2] and the dielectric relaxation in amorphous materials [3–5].

In the anomalous relaxation phenomena, the relaxation functions are expressed by nonexponential functions. Two types of empirical laws have been widely used to fit the experimental data concerning the anomalous relaxation: (i) the Cole-Cole form of the complex susceptibility in the frequency domain [6] and (ii) the stretched-exponential form of the relaxation function in the time domain [1,7]. From the fact that a large number of experimental data are described by a few simple empirical laws, it is expected that there must be common microscopic mechanisms in the anomalous relaxation observed in quite different kinds of phenomena.

With a view to clarifying microscopic mechanisms of the anomalous relaxation, we study the structural relaxation in normal and supercooled liquids. In particular, it is a purpose of this article to ascertain whether the anomalous structural relaxation is characteristic of the supercooled liquids which are in a metastable state, or it is universal in liquids in general irrespective of their thermodynamic states. To this end, we carry out the molecular-dynamics (MD) simulations of a Lennard-Jones binary mixture and study (1) the long-time behavior of the self-part of the number density autocorrelation function, which is the relaxation function in this case; and (2) the low-frequency behavior of the imaginary part of the self-part of the complex susceptibility at various temperatures and wave numbers systematically. As a result of our MD simulations, it is found that the anomalous structural relaxation appears even above the melting temperature T_m. In other words, the anomalous structural relaxation is shown to be a general phenomenon in liquids.

This paper is organized as follows: In Sec. II, we describe our model and method in detail. Our results obtained by MD simulations are presented in Sec. III. In Sec. IV, summary and discussions are given.

II. MODEL AND METHOD

The method of molecular-dynamics (MD) simulations is very useful in investigating not only the static properties but also the dynamical properties of liquids. This technique can yield a variety of correlation functions and single-particle motions in detail. Much work has been done in relation to the liquid-glass transition and some recent work can be found in Refs. [8–14].

We consider a binary mixture composed of N_1 atoms of mass m_1 and diameter $\sigma_1=\sigma$ and N_2 atoms of mass m_2 and diameter σ_2. Two atoms separated by distance r are supposed to interact through the Lennard-Jones potential

$$v_{\alpha\beta}(r)=4\epsilon\left[\left(\frac{\sigma_{\alpha\beta}}{r}\right)^{12}-\left(\frac{\sigma_{\alpha\beta}}{r}\right)^{6}\right], \tag{1}$$

where α and β are species indexes and equal to 1 or 2, while ϵ and $\sigma_{\alpha\beta}$ are parameters with dimensions of energy and length, respectively. The parameter $\sigma_{\alpha\beta}$ is assumed to satisfy

$$\sigma_{\alpha\beta}=\frac{1}{2}(\sigma_\alpha+\sigma_\beta). \tag{2}$$

In this paper, we choose $N_2/N_1=1.0$, $m_2/m_1=2.0$, and $\sigma_2/\sigma_1=1.2$. It is known that the system with these parameters bypasses crystallization, that is, the system stays in a supercooled state or a glassy state for a long time at a given temperature. As for the total number of particles N, we choose $N=500$ in cooling liquids. The microscopic time scale is chosen to be

$$\tau=\left(\frac{m_1\sigma^2}{48\epsilon}\right)^{1/2}. \tag{3}$$

When species 1 is assumed to be argon, we find $\tau=3.112\times10^{-13}$ s by substituting parameters appropriate for argon ($\epsilon/k_B=119.8$ K, k_B being the Boltzmann constant, $m_1=6.63\times10^{-26}$ kg and $\sigma=3.405$ Å) into Eq.(3). The value

*Present address: Theory and Computer Simulation Center, National Institute for Fusion Science, Nagoya 464-01, Japan.

of τ is comparable with the inverse of the Einstein frequency. In what follows, the temperature T is scaled by ϵ/k_B.

We systematically study the normal and supercooled liquids by constant-pressure MD simulations (Andersen's method [15]) in a cubic cell with periodic boundary conditions. We use the velocity version of the Verlet algorithm [16] and we take the time step $\Delta t/\tau = 0.07$.

III. RESULTS

A. Crystal structure

In this subsection, we derive the melting temperature T_m and the glass-transition temperature T_g of our Lennard-Jones system. In order to determine T_m, it is necessary to identify the crystal structure below T_m. In a one-component Lennard-Jones system, the crystal structure is known to be the face-centered cubic (fcc) structure. On the other hand, in a binary Lennard-Jones system, the type of the crystal structure depends on the ratio of diameters σ_2/σ_1. Since we have chosen the values of σ_2/σ_1 and m_2/m_1 so that crystallization is bypassed in a binary system, the crystal structure is not easily obtained by cooling liquids. As another way to determine a possible crystal structure of our binary Lennard-Jones mixture, we perform MD simulations starting from the following three initial configurations at a low enough temperature, say at $T=0.0835$; that is, (i) fcc structure obtained by placing alternatively two kinds of layers composed of face-centered squares, (ii) cesium chloride (CsCl) structure, and (iii) sodium chloride (NaCl) structure. Judging from the fact that the melting temperature T_m for a one-component Lennard-Jones system of an fcc structure is about 0.7, $T=0.0835$ is considered to be *low* in our binary system as well. (It is worth noting here that, when parameters σ and ϵ for a one-component Lennard-Jones system are taken to be appropriate for argon, T_m in the reduced scale corresponds to $T_m=84$ K while $T=0.0835$ to $T=10$ K.) The total number of particles in each structure is (i) $N=500$, (ii) 432, and (iii) 512. In Figs. 1(a), 1(b), and 1(c), the total pair distribution functions $g(r)$ versus interatomic distance r are shown by solid curves for the configurations resulting from these three MD simulations, respectively, while the broken curve in Fig. 1(c) corresponds to a glass obtained by quenching a liquid from $T=1.0017$ to $T=0.0835$. (Note that $T=1.0017$ in the reduced scale corresponds to $T=120$ K in the case of argon, the temperature being considered to be high enough for our purpose when compared to $T_m=84$ K.) The arrows in Figs. 1(a), 1(b), and 1(c), respectively, indicate the positions of the first eight nearest neighbors in an fcc lattice [Fig. 1(a)], the first nine nearest neighbors in a CsCl lattice [Fig. 1(b)], and the first nine nearest neighbors in an NaCl lattice [Fig. 1(c)]. From Figs. 1(a) and 1(b), it is found that the crystal structures of the fcc type and the CsCl type are stable. On the other hand, Fig. 1(c) ascertains that the NaCl structure is not stable and that the structure obtained from our MD simulations is more like a glass than like a crystal. In this way, the study of $g(r)$ suggests that either an fcc or a CsCl structure is a possible crystalline configuration for our model system. The next step, therefore, is to determine which of these two configurations is more preferable. For this purpose, we calculate the potential energy $E_{\rm pot}/N$ and volume V/N per particle at $T=0.0835$. The results are listed in Table I for the above-described two crystalline configurations as well as for a glass. From these results, it is obvious that the CsCl structure is most plausible out of the three configurations studied here.

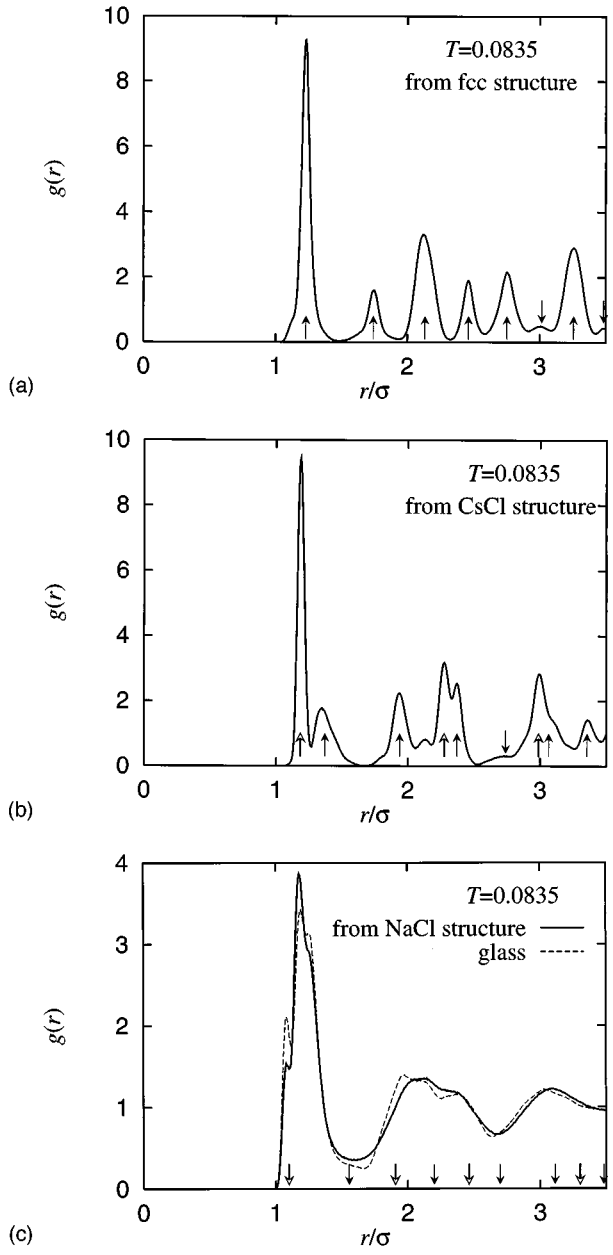

FIG. 1. The pair distribution functions $g(r)$ for the configurations resulting from the MD simulations starting from the following three initial configurations: (a) the fcc structure, (b) the CsCl structure and (c) the NaCl structure at $T=0.0835$. The pair distribution function $g(r)$ for a glass is also presented in (c). The arrows in (a), (b), and (c) show the positions of the first eight nearest neighbors in an fcc lattice, the first nine nearest neighbors in a CsCl lattice, and the first nine nearest neighbors in an NaCl lattice, respectively. In (b) and (c), the filled arrows represent the contributions from the partial distribution functions $g_{11}(r)$ and $g_{22}(r)$ and the open arrows denote the contributions from the partial distribution functions $g_{12}(r)$ and $g_{21}(r)$.

TABLE I. List of values of the potential energy per particle $E_{\rm pot}/N$ and the volume per particle V/N at $T=0.0835$ for two crystalline configurations resulting from the MD simulations and for a glass obtained by cooling liquids.

Configuration	$E_{\rm pot}/N$	V/N
fcc structure	-7.778	1.321
CsCl structure	-8.141	1.285
glass	-7.922	1.319

Now that a CsCl configuration is chosen as the crystal structure of our system, our task is to determine T_m and T_g of our system. Towards this end, we first heat this system from $T=0.0835$ to $T=1.0017$ (liquid) with the average heating rate 3.1×10^{10} Ks^{-1}. The specific volume V/N versus T for this heating process is plotted by filled circles in Fig. 2. From this figure, we see that the melting temperature is located around $T_m\simeq0.70$.

The liquid system at $T=1.0017$ obtained as a result of the above-described heating process is then cooled down to $T=0.0835$ with the average cooling rate 1.0×10^{9} Ks^{-1}. The open circles in Fig. 2 show the specific volume versus temperature in this cooling process. The glass-transition temperature is roughly estimated from the value at the intersection of the extrapolations both from the typical liquidlike and solidlike regions. The glass-transition temperature T_g thus determined is $T_g\simeq0.39$.

B. Structural relaxation

In this subsection, we clarify whether the structural relaxation is anomalous or not in the normal liquid state above the melting temperature by analyzing our MD results. We calculate the self-part of the number density autocorrelation functions $F_s^{(\alpha)}(k,t)$ and the imaginary part of the self-part of the complex susceptibilities $\chi_s^{(\alpha)\prime\prime}(k,\omega)$ relevant to the structural relaxation. These physical quantities are defined as follows:

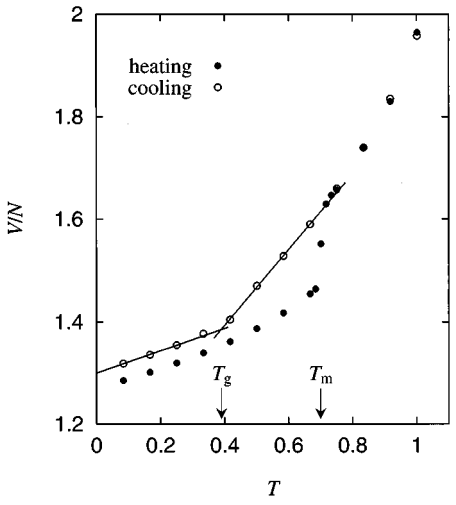

FIG. 2. The specific volume V/N versus temperature T in heating (filled circles) and in cooling (open circles). The solid lines represent the extrapolations in order to determine the glass transition temperature T_g. The melting temperature is $T_m\simeq0.70$ and the glass transition temperature is $T_g\simeq0.39$.

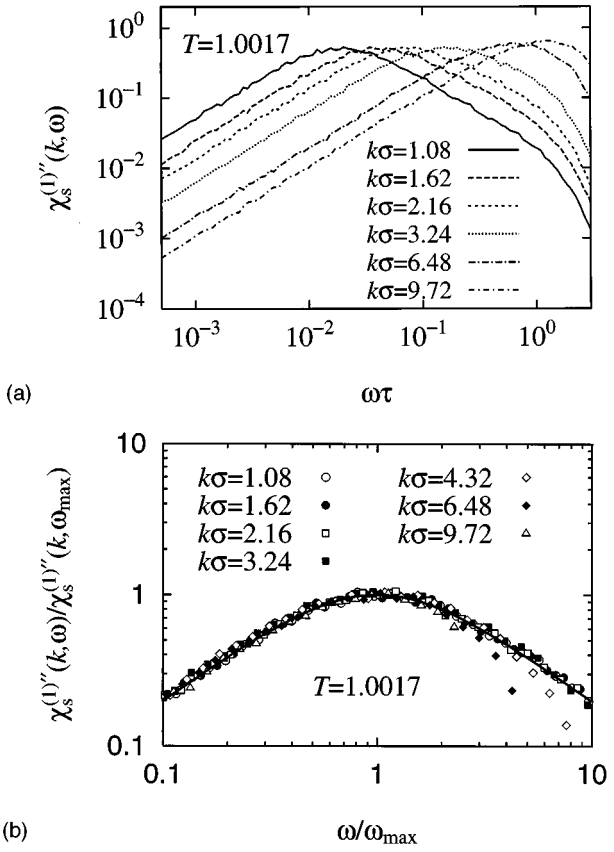

FIG. 3. (a) The imaginary part of the self-part of the complex susceptibility $\chi_s^{(1)\prime\prime}(k,\omega)$ for various wave numbers at $T=1.0017$. (b)$\chi_s^{(1)\prime\prime}(k,\omega)/\chi_s^{(1)\prime\prime}(k,\omega_{\rm max})$ versus $\omega/\omega_{\rm max}$ for various wave numbers at $T=1.0017$. The solid curve represents the Debye susceptibility.

$$F_s^{(\alpha)}(k,t)=\frac{1}{N_\alpha}\sum_{j=1}^{N_\alpha}\langle\exp\{i\mathbf{k}\cdot[\mathbf{r}_j^\alpha(t)-\mathbf{r}_j^\alpha(0)]\}\rangle, \tag{4}$$

$$\chi_s^{(\alpha)\prime\prime}(k,\omega)=\omega\int_0^\infty F_s^{(\alpha)}(k,t)\cos(\omega t)dt, \tag{5}$$

where $\mathbf{r}_j^\alpha(t)$ denotes the position vector of particle j of species α at time t, $\mathbf{k}$ is a wave number vector and $k\equiv|\mathbf{k}|$ is a wave number. The relaxation function $F_s^{(\alpha)}(k,t)$ contains information of the self-diffusion of particles.

Let us first study the behavior of a liquid at a temperature $T=1.0017$ which is as high as $T\simeq1.5T_m$. The reason why we start from a liquid at this temperature is that we like to make it sure that a liquid is *normal* at high enough temperature. In Fig. 3(a), the imaginary parts of the self-parts of the complex susceptibility $\chi_s^{(1)\prime\prime}(k,\omega)$ are shown for various wave numbers at this temperature. Note that at this temperature, the system is in an equilibrium state. From this figure, we find that the frequency of the peak becomes higher as the wave number becomes large. We show in Fig. 3(b) $\chi_s^{(1)\prime\prime}(k,\omega)/\chi_s^{(1)\prime\prime}(k,\omega_{\rm max})$ as a function of $\omega/\omega_{\rm max}$, where $\omega_{\rm max}$ is the frequency at which $\chi_s^{(1)\prime\prime}(k,\omega)$ has a peak. It is readily seen from this figure that scaling around $\omega=\omega_{\rm max}$ holds at small wave numbers and the structural relaxation is of the normal Debye type: i.e., $\chi_s^{(1)\prime\prime}(k,\omega)/$

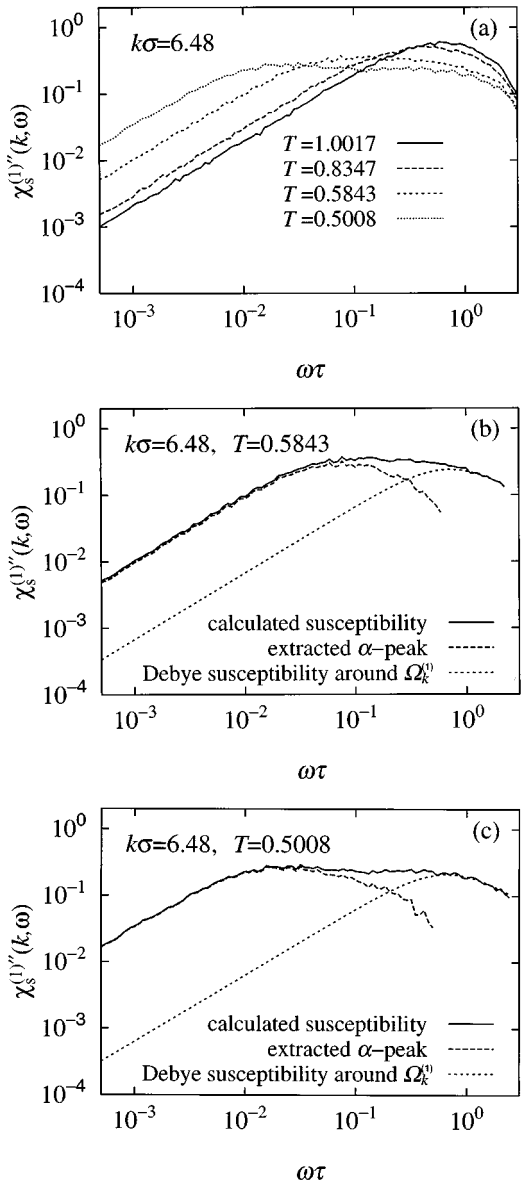

FIG. 4. (a) The imaginary part of the self-part of the complex susceptibility $\chi_s^{(1)''}(k,\omega)$ for various temperatures at $k\sigma=6.48$ which is the wave number of the main peak of the static structure factor. (b) At $T=0.5843$ and (c) at $T=0.5008$ (both for $k\sigma=6.48$), the appearance of the α peak (the broken curve) is ascertained by subtracting the Debye peak around the microscopic frequency $\Omega_k^{(1)}$ (the dotted curve) from the total susceptibility $\chi_s^{(1)''}(k,\omega)$ (the solid curve) obtained from our simulations.

$\chi_s^{(1)''}(k,\omega_{\max})=\mathrm{Im}\,[(1-i\omega/\omega_{\max})^{-1}]$ (solid curve in this figure) as is normally expected for a normal liquid above T_m. On the other hand, at large wave numbers, the normalized susceptibilities $\chi_s^{(1)''}(k,\omega)/\chi_s^{(1)''}(k,\omega_{\max})$ at high frequencies are located under the solid curve. This fact indicates that the structural relaxation at high frequencies is *faster* than the Debye relaxation, and consequently a liquid is ''*not perfectly normal*'' *even at a high enough temperature.*

In the next place, let us study the behavior of a liquid at temperatures lower than $T=1.0017$. The imaginary parts of the self-part of the complex susceptibility $\chi_s^{(1)''}(k,\omega)$ are shown in Fig. 4(a) for various temperatures at the wave number $k\sigma=6.48$, which corresponds to the wave number of the main peak of the static structure factor. From this figure, we can see the following facts: (a) At high temperature $T=1.0017$, $\chi_s^{(1)''}(k,\omega)$ has only one peak at the microscopic frequency ($\omega\tau\approx1$). (b) As the temperature is reduced, the width of the peak becomes broader towards the low-frequency side even above T_m, which suggests the appearance of an additional peak at the low-frequency side. (c) When the temperature is reduced beyond $T\simeq0.5$, an additional peak appears at the low-frequency side. The appearance of ''*the low-frequency peak*'' can be clearly seen by subtracting the Debye peak centered around the microscopic frequency $\Omega_k^{(1)}$ from the calculated $\chi_s^{(1)''}(k,\omega)$ [Figs. 4(b) and 4(c)], where

$$\Omega_k^{(1)}=k\left(\frac{k_BT}{m_1}\right)^{1/2}. \tag{6}$$

These facts suggest that the structural relaxation becomes anomalous even above T_m. We also find from Figs. 4(b) and 4(c) that the frequency at the maximum position of ''*the low-frequency peak*'' decreases rather drastically as the temperature decreases while the frequency $\Omega_k^{(1)}$ at the maximum position of the Debye susceptibility has a relatively weak dependence on the temperature as defined by Eq. (6). A remarkable temperature dependence is one of the characteristic features of the so-called α peak observed in supercooled liquids. Therefore, it is expected that the peak at the low-frequency side [broken curves in Figs. 4(b) and 4(c)] corresponds to the α peak.

In order to study the structural relaxation in the low-frequency region or in the long-time region in more detail, we analyze the self-parts of the number density autocorrelation functions. The self-parts of the number density autocorrelation function $F_s^{(1)}(k,t)$ are shown in Fig. 5 for various temperatures and wave numbers. In the time region ($t/\tau>3.5$) longer than the microscopic time scale ($t/\tau\approx1$), the self-parts $F_s^{(1)}(k,t)$ are well fitted by the stretched-exponential function

$$F_s^{(1)}(k,t)\sim A^{(1)}\exp\left[-\left(\frac{t}{\tau^{(1)}}\right)^{\beta^{(1)}}\right]\quad(t/\tau>1), \tag{7}$$

where $\tau^{(1)}$ is the relaxation time and $\beta^{(1)}$ is the stretching parameter which represents the degree of stretching of the relaxation. The fact that the long-time parts of $F_s^{(1)}(k,t)$ are fitted by the stretched-exponential function is another characteristic feature of the α peak. Thus the relaxation in the long-time region or in the low-frequency region is ascertained to be the α peak as is expected in the above.

We show the relaxation time as a function of the inverse temperature in Fig. 6. In Figs. 7 and 8 are shown the stretching parameters as a function of temperature and as a function of the wave number, respectively. As seen in Fig. 6, Arrhenius behavior is observed in the temperature region above T_m. From this fact, we can say that a liquid above T_m is normal not only in the ordinary thermodynamical sense but also in the sense that the relaxation time obeys a normal Arrhenius law. On the other hand, from Figs. 7 and 8, we find that (a) at small wave numbers ($k\sigma\leqslant2.16$), the stretch-

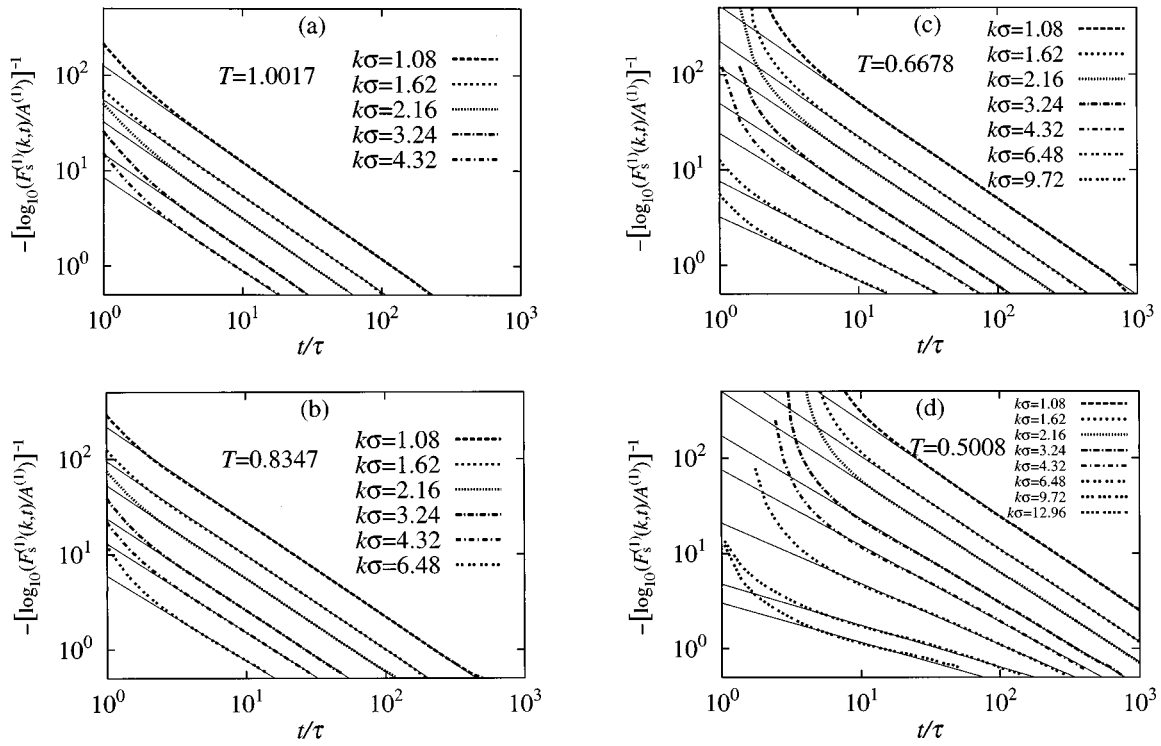

FIG. 5. The self-part of the number density autocorrelation functions scaled by $A^{(1)}$, $F_s^{(1)}(k,t)/A^{(1)}$, for various wave numbers at (a) $T=1.0017$, (b) $T=0.8347$, (c) $T=0.6678$, and (d) $T=0.5008$. The solid curves represent the curves fitted by the stretched-exponential function [Eq.(7)].

ing parameter $\beta^{(1)}$ is almost unity, (b) at large wave numbers ($k\sigma \geqslant 2.16$), $\beta^{(1)}$ is less than unity even above T_m, (c) at large wave numbers ($k\sigma \geqslant 2.16$), $\beta^{(1)}$ decreases as the temperature decreases at a given wave number and as the wave number increases at a given temperature. This fact (c) indicates that the structural relaxation becomes slower as the temperature decreases or as the wave number increases. The stretching parameters $\beta^{(1)}$ at $k\sigma=6.48$, where the imaginary parts $\chi_s^{(1)\prime\prime}(k,\omega)$ are shown for several temperatures in Fig. 4, are shown by filled diamonds in Fig. 7. It is clearly found that the stretching parameter $\beta^{(1)}$ is found to be less than unity even at higher temperatures than the melting temperature T_m.

IV. SUMMARY AND DISCUSSION

In this article, we have studied the structural relaxation in many-body systems such as a binary Lennard-Jones system by MD simulations.

(i) The crystal structure of our binary Lennard-Jones system is a CsCl structure. The melting temperature is $T_m \simeq 0.70$ and the glass-transition temperature $T_g \simeq 0.39$.

(ii) At a temperature $T \simeq 1.5T_m$ which is considered to be high enough, the imaginary part of the self-parts of the complex susceptibility $\chi_s^{(1)\prime\prime}(k,\omega)$ versus frequency ω indicates that there exist deviations from the normal Debye relaxation at high frequencies.

(iii) In a liquid at temperature T between T_m and

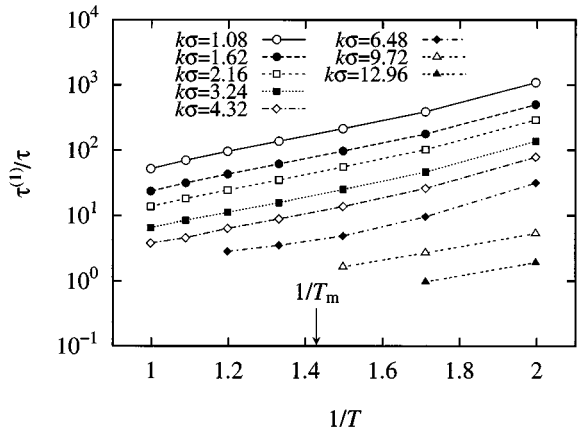

FIG. 6. The relaxation time $\tau^{(1)}$ versus inverse temperature $1/T$ for various wave numbers.

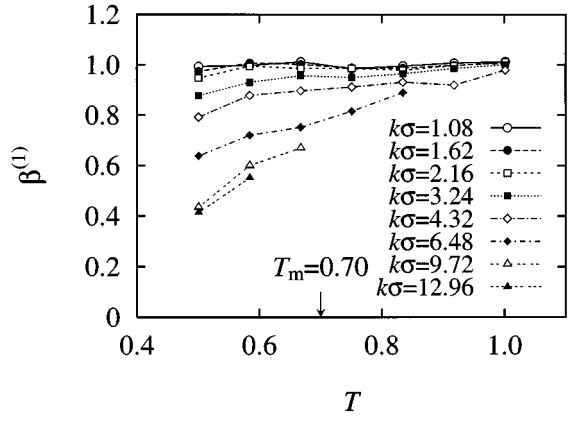

FIG. 7. The stretching parameter $\beta^{(1)}$ versus temperature T for various wave numbers.

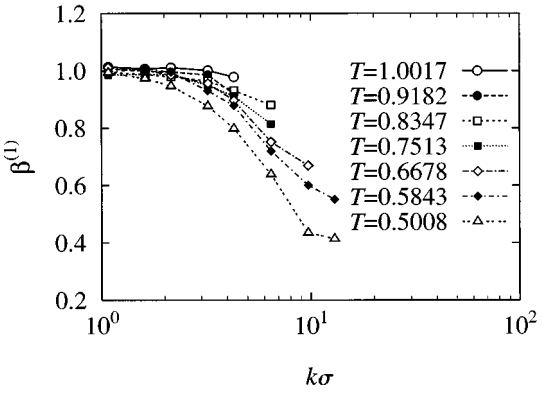

FIG. 8. The stretching parameter $\beta^{(1)}$ versus wave number k for various temperatures.

$1.5T_m$, the structural relaxation in the long-time region is of the stretched-exponential type in spite of the fact that the system has several features characteristic of normal liquids such as the Arrhenius behavior of the relaxation time and the thermodynamic behavior concerning the equations of state.

(iv) In the temperature region as described in (iii), i.e., in the region $T_m<T<1.5T_m$, the stretching parameter β decreases as the temperature reduces and as the wave number increases.

The results similar to our results presented in Fig. 7 have also been indicated experimentally in the structural relaxation in an ionic glass former $[Ca(NO_3)_2]_{0.4}[K(NO_3)]_{0.6}$ (CKN) (Fig. 3 in Ref. [17]) and in the mechanical relaxation in CKN (Fig. 6 in Ref. [18]); that is, we can read that the stretching parameter is less than unity even above the melting temperature T_m when we look at these experimental results closely. Moreover, in Ref. [18], Campbell *et al.* suggest that another characteristic temperature, which is identified with the Griffith temperature in the spin-glass context, should exist for which the relaxation becomes exponential. In our MD simulations, this characteristic temperature is found to exist and increase according to the increase of the wave number as shown in Figs. 7 and 8. The fact that the anomalous relaxation appears even in the so-called normal liquid was suggested experimentally by Ngai and Strom [19]. In this paper, we have confirmed this fact by means of the systematic study by the computer simulations.

Here we discuss the finite-size effect. The linear dimension R corresponding to the smallest wave number we studied, i.e., $k\sigma=1.08$, is $R/\sigma=2\pi/k\sigma\sim5.8$, which is the largest linear dimension we are concerned with in our simulations. On the other hand, the linear system size $V^{1/3}$ in the temperature region between $T=0.5$ to $T=1.0$ is $V^{1/3}\sigma=9.0\sim9.9$. Consequently, the finite-size effect is expected to be very small since $R<V^{1/3}$.

A most remarkable conclusion drawn from our study is that the structural relaxation becomes anomalous not only in supercooled liquids but also in the normal liquid region. The conclusion achieved in this article indicates that the anomalous structural relaxation is closely related to the disordered nature in a system.

Before concluding this paper, let us mention that, as a model of the structural relaxation, we previously proposed a one-body picture: i.e., ''random walks in restricted geometry'' and made detailed study of the relation between the anomalous relaxation and the nature of disorder in systems with restricted geometry [20–22]. Note also that Flesselles and Botet have investigated the stretched-exponential anomalous relaxation analytically through random walks on a percolating network, modelizing the available phase space of a disordered material [23].

ACKNOWLEDGMENT

The authors are grateful for valuable discussions with Dr. S. Gomi.

[1] R. Kohlrausch, Ann. Phys. (Leipzig) **12**, 393 (1847).
[2] W. Götze, *Liquids, Freezing and Glass Transition*, edited by J.-P. Hansen, D. Levesque, and J. Zinn-Justin (North-Holland, Amsterdam, 1991).
[3] H. Scher, M. F. Shlesinger, and J. T. Bendler, Phys. Today **44**, 26 (1991).
[4] J. Kakalios, R. A. Street, and W. B. Jackson, Phys. Rev. Lett. **59**, 1037 (1987).
[5] Y. Fujita, M. Yamaguchi, and K. Morigaki, Philos. Mag. B **69**, 57 (1994).
[6] K. S. Cole and R. H. Cole, J. Chem. Phys. **9**, 341 (1941).
[7] G. Williams and D. C. Watts, Trans. Faraday Soc. **66**, 80 (1970).
[8] B. Bernu, J.-P. Hansen, Y. Hiwatari, and G. Pastore, Phys. Rev. A **36**, 4891 (1987).
[9] H. Miyagawa, Y. Hiwatari, B. Bernu, and J.-P. Hansen, J. Chem. Phys. **88**, 3879 (1988).
[10] G. Pastore, B. Bernu, J.-P. Hansen, and Y. Hiwatari, Phys. Rev. A **38**, 454 (1988).
[11] G. Wahnström, Phys. Rev. A **44**, 3752 (1991).
[12] G. Wahnström, J. Non-Cryst. Solids **131-133**, 109 (1991).
[13] Y. Hiwatari, J. Matsui, K. Uehara, T. Muranaka, H. Miyagawa, M. Takasu, and T. Odagaki, Physica A **204**, 306 (1994).
[14] F. Yonezawa and S. Fujiwara, Mater. Sci. Eng. A **178**, 23 (1994).
[15] H. C. Andersen, J. Chem. Phys. **72**, 2384 (1980).
[16] L. Verlet, Phys. Rev. **159**, 98 (1967).
[17] L. Börjesson, M. Elmroth, and L. M. Torell, J. Non-Cryst. Solids **131-133**, 139 (1991).
[18] I. A. Campbell, J.-M. Flesselles, R. Jullien, and R. Botet, Phys. Rev. B **37**, 3825 (1988).
[19] K. L. Ngai and U. Strom, Phys. Rev. B **27**, 6031 (1983).
[20] S. Fujiwara, S. Gomi, K. Morigaki, and F. Yonezawa, J. Non-Cryst. Solids **164-166**, 301 (1993).
[21] S. Fujiwara and F. Yonezawa, Phys. Rev. Lett. **74**, 4229 (1995).
[22] S. Fujiwara and F. Yonezawa, Phys. Rev. E **51**, 2277 (1995).
[23] J. M. Flesselles and R. Botet, J. Phys. A **22**, 903 (1989).